Gold Nanoprobes

DOI: 10.1002/anie.200705240

A Near-Infrared-Fluorescence-Quenched Gold-Nanoparticle Imaging Probe for In Vivo Drug Screening and Protease Activity Determination**

Seulki Lee, Eui-Joon Cha, Kyeongsoon Park, Seung-Young Lee, Jin-Ki Hong, In-Cheol Sun, Sang Yoon Kim, Kuiwon Choi, Ick Chan Kwon, Kwangmeyung Kim, and Cheol-Hee Ahn**

Nanoscale fluorescence optical imaging probes are paving the way for novel methods to sense and spot live molecular targets.[1] Various probes have been developed, including semiconductor quantum dots,[2] magnetofluorescent nanoparticles,[3] polymer conjugates,[4] nanocomplexes,[5] and gold nanoparticles (AuNPs).[6] The application of conventional fluorescent probes is limited because they generally display only modest fluorescence changes, thus providing insufficient resolution. The limited degree of resolution is mainly attributed to the low fluorescence-quenching efficiency and specificity of the probes. Therefore, a high quenching efficiency and specific recognition properties by the target biomolecules are essential for the development of supersensitive fluorescence-based probes. Among the diverse candidates, biocompatible AuNPs[7] offer a considerable advantage in obtaining optical images through their near-infrared-fluorescence (NIRF) quenching properties. Chromophores in close proximity to AuNPs experience strong electronic interactions with the surface, which results in donation of excited electrons to the metal nanoparticles and almost perfect quenching of the fluorescence.[8] However, the use of AuNP probes for in vivo visual biomolecular detection and real-time fluorescence tomography remains to be explored.

[*] Dr. S. Lee,[+] Dr. K. Park, S.-Y. Lee, Dr. K. Choi, Dr. I. C. Kwon, Dr. K. Kim
Biomedical Research Center
Korea Institute of Science and Technology
39-1 Hawolgok-dong, Seongbuk-gu, Seoul, 136-791 (Korea)
Fax: (+82) 2-958-5909
E-mail: kim@kist.re.kr
E.-J. Cha,[+] J.-K. Hong, I.-C. Sun, Prof. C.-H. Ahn
Department of Materials Science and Engineering
Seoul National University
San 56-1, Sillim, Gwanak, Seoul 151-744 (Korea)
Fax: (+82) 2-883-8197
E-mail: chahn@snu.ac.kr
S. Y. Kim
Asan Medical Center, School of Medicine
Ulsan University, 388-2 Pungnap2-dong
Songpa-gu, Seoul, 138-736 (Korea)
[+] These authors contributed equally to this work.

[**] This work was financially supported by the Real-Time Molecular Imaging Project and Global Research Laboratory Program of MOST and Intramural Research Program of the KIST.
Supporting information for this article is available on the WWW under http://www.angewandte.org or from the author.

Herein, we describe the development of a protease-sensitive self- and AuNP-quenched NIRF probe. Proteases—or their inhibitors—are mainly involved in cancer, inflammation, and vascular disease.[9] Sensitive, convenient, and accurate protease-detection systems constitute a crucial tool for the development of drug-screening systems and the early diagnosis of diseases, such as cancer. The most common detection method for protease activity is the use of small peptide substrates containing chromophores at their termini. We previously reported protease- and kinase-activating sensory systems based on the fluorescence resonance energy transfer (FRET) properties of NIRF Cy or isothiocyanate dyes.[4a,5] Although these systems are sensitive, their applications are limited because of the modest fluorescent changes (which are too weak to be used in vivo). Therefore, a decrease in the noise intensity of the quenched state—to an undetectable level—is required to maximize the fluorescent changes and achieve an efficient in vivo detection of small amounts of protease. Herein, we propose an alternative, simple, robust, and one-step optical fluorescence nanoprobe to be used in: 1) inhibitor drug screening, 2) the detection of target proteases, and 3) the early diagnosis of cancer.

The system Cy5.5-substrate/AuNP is believed to induce a strong multi-quenched state, because the AuNPs serve as ultra-efficient quenchers of the molecular excitation energy in a chromophore through their surface-energy-transfer properties,[7,8a] and the Cy5.5 dye, loaded onto the AuNP surfaces, can be self-quenched as a result of a combination of the static-quenching and FRET mechanisms.[10] When the target proteases meet functionalized AuNP probes, cleavage of the Cy5.5-substrate occurs as a consequence of the specific substrate recognition by the protease. This cleavage is manifested in the form of a pronounced NIRF signal recovery caused by dequenching of the NIRF dyes (Figure 1A). To demonstrate the utility of our rationale, we developed a matrix metalloprotease (MMP) fluorescence imaging probe based on AuNPs. MMPs are a family of zinc-dependent endopeptidases that play key roles in several biological processes.[11] In particular, because of their significant role in promoting cancer progression, MMPs have become important targets for new drug development and in vivo tumor diagnosis.

We prepared AuNPs (20 nm) stabilized with a Cy5.5-substrate, namely, Cy5.5-Gly-Pro-Leu-Gly-Val-Arg-Gly-Cys-(amide), where the core-specific substrate, that is, Pro-Leu-Gly-Val-Arg, shows selectivity for MMP (see the Supporting Information).[4b] Transmission electron microscopy (TEM)

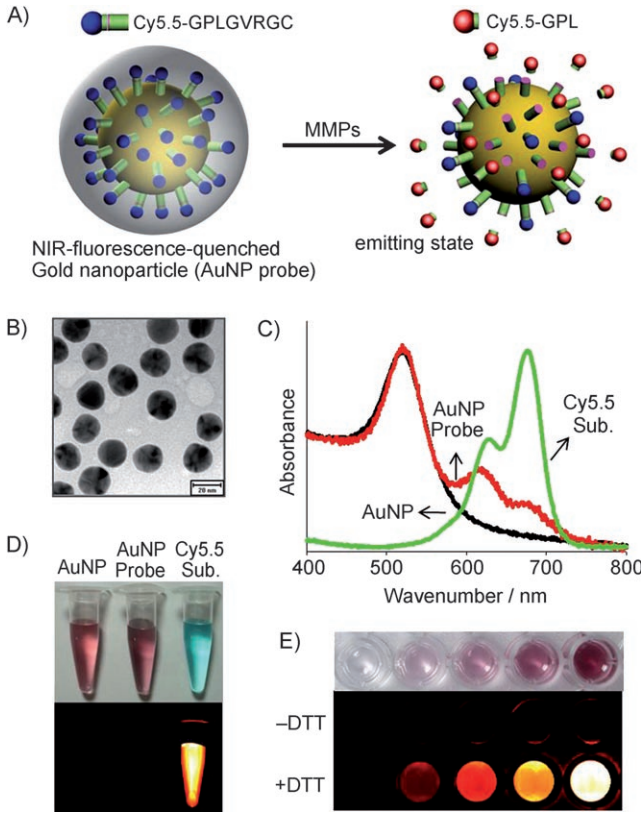

Figure 1. A) The MMP-sensitive AuNP probe. B) TEM image of the AuNP probe. C) UV/Vis spectra of AuNP, AuNP-probe, and Cy5.5-substrate solutions. D) Bright and NIRF image of vials containing AuNP, AuNP-probe, and Cy5.5-substrate solutions. E) Bright and NIRF image sections of a 96-well microplate containing 0, 2.7, 7, 14, and 27 nM of the AuNP probes (left to right) with and without DTT.

images reveal uniform functionalized AuNPs with an average size of about 20 nm (Figure 1B). The AuNP-probe solutions were analyzed by means of UV/Vis spectroscopy, thereby exhibiting plasmon bands for the AuNPs and Cy5.5 (Figure 1C). The AuNP probes were well dispersed in the reaction buffer (composed of 100 mM Tris, 5 mM calcium chloride, 200 mM NaCl, 0.1% Brij, and 0.02% poly(ethylene glycol) (PEG) M_w 20 kDa), and the NIRF signals were completely quenched when visualized with a Kodak image station 4000MM equipped with filter systems for Cy5.5 (Figure 1D). The quenching properties of the AuNP probes were also visualized using the Kodak image station. As shown in Figure 1E, increased concentrations of the AuNP probes in the wells did not affect the background NIRF signal. However, addition of 1,4-dithiothreitol (DTT) caused a displacement of the Cy5.5-substrate from the AuNPs, which resulted in an enhanced NIRF-signal recovery that was dependent on the AuNP-probe concentration. Furthermore, fluorescence titration was conducted (using a spectrofluorometer) to determine the amount of Cy5.5-substrate bound to the AuNP surface. The NIRF intensity of Cy5.5 was calibrated and the concentration of bound Cy5.5-substrate was determined from known concentrations of DTT-treated AuNPs. DTT displacement of the Cy5.5-substrate from the AuNPs resulted in a significant (about 120-fold) increase of the NIRF signals. We estimated concentrations of 114 ± 3 molecules of Cy5.5-substrate per AuNP. The quenching efficiency (QE, [%]) of the AuNPs was calculated by using the formula: $100 \times (1\text{-}\beta)$, where β is the ratio of fluorescence of the quenched-to-completely dequenched state. The QE of a single AuNP was calculated to be 99.17 ± 0.12.

The enzyme selectivity of the AuNP probes was evaluated in vitro by incubation in a cuvette containing the reaction buffer and 14 nmol L^{-1} of activated MMP-2, MMP-3, MMP-7, MMP-13, MMP-2 containing AuNP probes decorated with a Cy5.5–scramble peptide (containing the same peptide in a different sequence) or MMP-2 with an inhibitor. After incubation for 120 min with the respective enzymes and the inhibitor (at 37 °C), the NIRF emission signals of the samples were measured at a fixed excitation wavelength of 675 nm. Simultaneously, each sample was moved to a 96-well microplate and directly placed in the Kodak image station. As shown in Figure 2A, B, the AuNP probes were able to recover strong NIRF signals against various MMPs (approximately 13.9, 12.2, 16.5, and 24.4-fold for MMP-2, -3, -7, and -13, respectively). In contrast, no NIRF signals were recovered upon exposure of the AuNP probes containing the scramble control substrate to purified MMP-2. Furthermore, recovery of the NIRF signals by the AuNP probes was strongly disrupted (3.3-fold) in the presence of the MMP-2 inhibitor. Among the various MMPs, measurements were performed using the same experimental setup with different concentrations of activated MMP-2 (namely, 1, 3, 7, and 14 nmol L^{-1}, see Figure 2C). A proportional relationship was observed between the MMP-2 concentration and the recovered NIRF signal. Furthermore, this procedure can be simply visualized as NIRF images (Figure 2D), which supports the effective use of the AuNP probes for the quantitative and visual analysis of the activity and function of protease. The degradation susceptibility of bound Cy5.5-substrate decreased as a result of the steric-hindrance induced by the bulky AuNPs.[6c] It was calculated that 28.45 ± 1.51% of the NIRF signals were recovered by MMP-2 from the total bound peptide on the AuNPs. We then examined the potential biological toxicity of the AuNP probes. Our in vitro cellular toxicity studies showed that in terms of biocompatibility, the AuNP probes are nontoxic (see the Supporting Information). However, the in vivo chronic toxicity of the probes must be thoroughly investigated because larger AuNPs (with sizes above 5.5 nm) could not be efficiently cleared by renal excretion in previous studies.[12]

Mice bearing SCC7 tumors (SCC7: squamous cell carcinoma, MMP-2 expression in the tumor cell lines) were selected as the animal model. The SCC7 cell lines were used because of the higher MMP-2 expression (observed by means of zymography) relative to that of the putative MMP-2-overexpressing cell lines, HT1080[13] (see the Supporting Information). In vivo imaging of subcutaneous-SCC7-tumor-xenografted mice was performed at 30, 60, 120, and 240 min after injection of the AuNP probes (with and without MMP-2 inhibitor) using the preclinical optical imaging system eXplore Optix (ART, Montreal, Canada), which was configured for NIRF probe detection (excitation and emission at

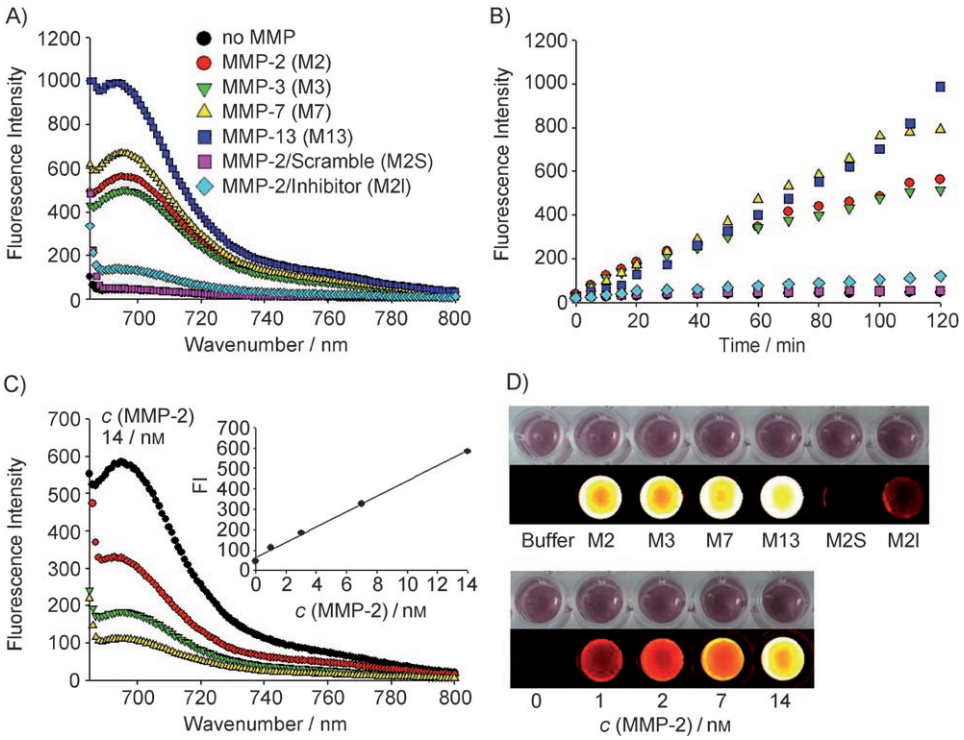

Figure 2. A) NIRF emission spectra of AuNP probes in the presence of various stimuli (14 nmol L^{-1} of activated MMP-2, -3, -7, -13, and MMP-2 with inhibitor) following incubation for 120 min at 37 °C. B) Fluorescence intensity of an AuNP probe as a function of time at 37 °C. C) Fluorescence emission spectra of AuNP probes in the presence of various concentrations of MMP-2 following incubation for 120 min at 37 °C. Inset: MMP-2 standard curve. D) Corresponding bright and NIRF image sections of a 96-well microplate of the AuNP probes containing various stimuli (top) and MMP-2 concentrations (bottom).

670 and 700 nm, respectively). Imaging was performed for 4 h after injection of the AuNP probes, and the images were assessed using an analysis workstation (ART Advanced Research Technologies Inc.). Details of the imaging system and associated mathematical image reconstructions are described in a previous report.[14] Figure 3 A depicts a series of typical NIRF images of athymic nude mice—with and without SCC7 tumors (between 5 and 7 mm)—obtained for 240 min after the intratumoral injection of the AuNP probes. Upon injection of the probes into the backs of normal athymic nude mice, the NIRF signal intensity did not vary substantially from that of the surrounding background tissue. On the other hand, in the case of tumor-bearing mice, the AuNP probes produced a high NIRF signal intensity, thus enabling clear visualization. However, tumor contrast was significantly reduced when the MMP-2 inhibitor was administered 30 min before injection of the AuNP probe.

To further characterize the increased NIRF signals in the tumor region, the tumors were excised and analyzed using a Kodak image station (Figure 3 B). The total NIRF signal of the tumors excised from the animals treated with the AuNP probes was stronger than that of the inhibitor-treated animals, which is consistent with the in vivo imaging data. Next, we analyzed selected tumor sections (Figure 3 C). Hematoxylin/eosin and anti-MMP-2 antibody staining revealed the presence of multiple mitotic figures in the proliferating SCC7 carcinoma as well as a strong MMP-2 expression in the SCC7 tumors. The results of

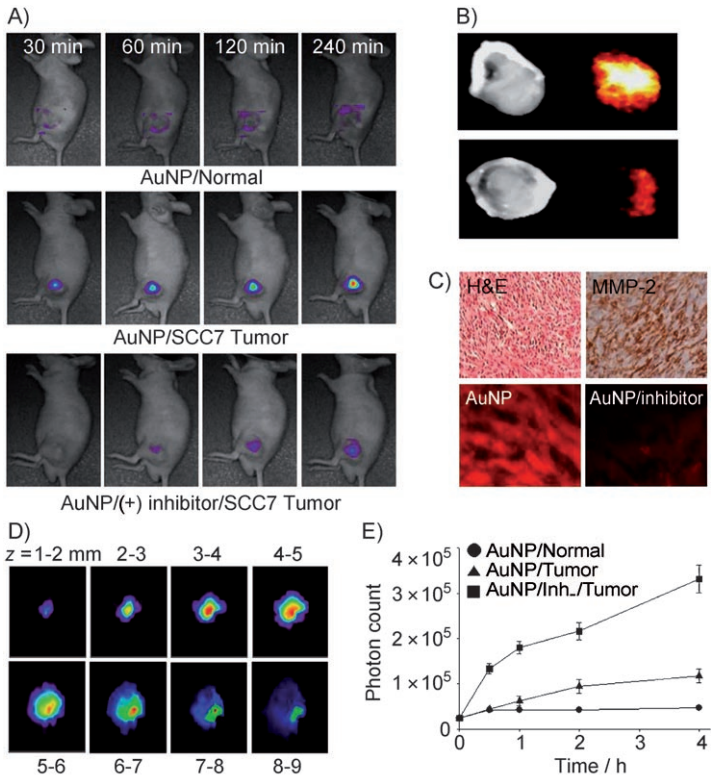

Figure 3. A) NIRF tomographic images of normal and subcutaneous-SCC7-tumor-bearing mice after injection of the AuNP probe with and without inhibitor (blue: low intensity, red: high intensity). B) NIRF images of excised AuNP-probe-treated SCC7 tumors with and without MMP-2 inhibitor. C) Immunohistology results for SCC7 tumors with MMP-2. H&E = Hematoxylin/eosin stain; lower row: NIRF microscopy of SCC7 tumors containing AuNP probes without and with inhibitor. D) 2D slices of the image from (A) reconstructed in the *z* direction (blue: low concentration, red: high concentration). E) Quantitative image analysis performed by counting the total number of photons in the tumors as a function of time.

NIRF imaging were confirmed by means of fluorescence microscopy, which revealed a significant difference between the two groups. Furthermore, images were constructed showing the intensity in slices cut along the z axis (Figure 3A) and represented in the form of 2D slices (Figure 3D). The total photon counts in tumoral and normal tissues as a function of time for each case are depicted in Figure 3E. An increased NIRF intensity ratio between the tumoral and normal tissues (T/N) was detected as early as 30 min after injecting the AuNP probes. This ratio gradually increased (up to 7.0 ± 0.6 at 240 min), whereas the inhibitor-treated tissue presented a significantly reduced T/N value (of 2.5 ± 0.3). Unfortunately, intravenously injected AuNP probes did not show increased NIRF signals in the tumor region. Moreover, it has been reported that intravenously injected AuNPs with larger sizes (that is, greater than 5.5 nm) may lead to precipitation and clearance from the bloodstream because of uptake by the liver.[12,15] Therefore, we are currently undertaking measures to further improve the AuNP probes by reducing the size of the antibiofouling surfaces and the tumor targeting moieties. Our results collectively confirm the feasibility of using the new AuNP probes for the in vitro and in vivo detection and visualization of targeted MMP-2—following intratumoral injection—in MMP-2-positive tumor-bearing mice.

The AuNP-based multi-quenched NIRF probes allow a simple visual monitoring of the activities of both protease and the inhibitor (in vitro and in vivo). Moreover, this platform can be applied to any target protease by using the appropriate peptide substrate spacer. Our AuNP-based fluorescent-probe system does not require expensive instrumentation and is able to identify target proteases in a rapid and efficient fashion—both in vitro and in vivo. The outstanding properties of this system highlight its potential as a novel molecular imaging probe.

Received: November 14, 2007
Revised: December 18, 2007
Published online: February 27, 2008

Keywords: cancer diagnosis · drug screening · fluorescent probes · gold · imaging agents

[1] a) R. Weissleder, V. Ntziachristos, *Nat. Med.* **2003**, *9*, 123–128; b) I. L. Medintz, H. T. Uyeda, E. R. Goldman, H. Mattoussi, *Nat. Mater.* **2005**, *4*, 435–446.
[2] a) S. Kim, Y. T. Lim, E. G. Soltesz, A. M. De Grand, J. Lee, A. Nakayama, J. A. Parker, T. Mihaljevic, R. G. Laurence, D. M. Dor, L. H. Cohn, M. G. Bawendi, J. V. Frangioni, *Nat. Biotechnol.* **2004**, *22*, 93–97; b) X. Michalet, F. F. Pinaud, L. A. Bentolila, J. M. Tsay, S. Doose, J. J. Li, G. Sundaresan, A. M. Wu, S. S. Gambhir, S. Weiss, *Science* **2005**, *307*, 538–544; c) X. Gao, L. Yang, J. A. Petros, F. F. Marshall, J. W. Simons, S. Nie, *Curr. Opin. Biotechnol.* **2005**, *16*, 63–72.
[3] a) L. Quinti, R. Weissleder, C. H. Tung, *Nano Lett.* **2006**, *6*, 488–490; b) W. S. Seo, J. H. Lee, X. Sun, Y. Suzuki, D. Mann, Z. Liu, M. Terashima, P. C. Yang, M. V. McConnell, D. G. Nishimura, H. Dai, *Nat. Mater.* **2006**, *5*, 971–976.
[4] a) K. Kim, M. Lee, H. Park, J. H. Kim, S. Kim, H. Chung, K. Choi, I. S. Kim, B. L. Seong, I. C. Kwon, *J. Am. Chem. Soc.* **2006**, *128*, 3490–3491; b) C. Bremer, C. H. Tung, R. Weissleder, *Nat. Med.* **2001**, *7*, 743–748; c) V. Ntziachristos, C. H. Tung, C. Bremer, R. Weissleder, *Nat. Med.* **2002**, *8*, 757–760.
[5] J. H. Kim, S. Lee, K. Park, H. Y. Nam, S. Y. Jang, I. Youn, K. Kim, H. Jeon, R. W. Park, I. S. Kim, K. Choi, I. C. Kwon, *Angew. Chem.* **2007**, *119*, 5881–5884; *Angew. Chem. Int. Ed.* **2007**, *46*, 5779–5782.
[6] a) S. I. Stoeva, J. S. Lee, J. E. Smith, S. T. Rosen, C. A. Mirkin, *J. Am. Chem. Soc.* **2006**, *128*, 8378–8379; b) C. Guarise, L. Pasquato, V. De Filippis, P. Scrimin, *Proc. Natl. Acad. Sci. USA* **2006**, *103*, 3978–3982; c) N. L. Rosi, D. A. Giljohann, C. S. Thaxton, A. K. Lytton-Jean, M. S. Han, C. A. Mirkin, *Science* **2006**, *312*, 1027–1030; d) C. C. You, O. R. Mirandra, B. Gider, P. S. Ghosh, I-B. Kim, B. Erdogan, S. A. Krovi, U. H. F. Bunz, V. M. Rotello, *Nat. Nanotechnol.* **2007**, *2*, 318–323.
[7] E. E. Connor, J. Mwamuka, A. Gole, C. J. Murphy, M. D. Wyatt, *Small* **2005**, *1*, 325–327.
[8] a) B. Dubertret, M. Calame, A. J. Libchaber, *Nat. Biotechnol.* **2001**, *19*, 365–370; b) C. S. Yun, A. Javier, T. Jennings, M. Fisher, S. Hira, S. Peterson, B. Hopkins, N. O. Reich, G. F. Strouse, *J. Am. Chem. Soc.* **2005**, *127*, 3115.
[9] D. R. Edwards, G. Murphy, *Nature* **1998**, *394*, 527.
[10] M. K. Johansson, R. M. Cook, *Chem. Eur. J.* **2003**, *9*, 3466–3471.
[11] M. Egeblad, Z. Werb, *Nat. Rev. Cancer* **2002**, *2*, 161–174.
[12] H. Soo Choi, W. Liu, P. Misra, E. Tanaka, J. P. Zimmer, B. I. Ipe, M. G. Bawendi, J. V. Frangioni, *Nat. Biotechnol.* **2007**, *25*, 1165–1170.
[13] C. Bremer, S. Bredow, U. Mahmood, R. Weissleder, C. H. Tung, *Radiology* **2001**, *221*, 523–529.
[14] S. Bloch, F. Lesage, L. McIntosh, A. Gandjbakhche, K. Liang, S. Achilefu, *J. Biomed. Opt.* **2005**, *10*, 054003.
[15] D. Kim, S. Park, J. H. Lee, Y. Y. Jeong, S. Jon, *J. Am. Chem. Soc.* **2007**, *129*, 7661–7665.

